10.1109/ULTSYM.2014.0475

Ultra-High Frequency Acoustic Impedance Maps of MCF-7 Cells

Muhannad N. Fadhel, Elizabeth S. L. Berndl, Eric M. Strohm and Michael C. Kolios*
Department of Physics
Ryerson University
Toronto, Ontario
mkolios@ryerson.ca

***Abstract*—Acoustic impedance maps can be used to gain an insight into the microstructure and physiological state of cancer cells. In this we correlated acoustic impedance maps with cells structures detected by fluorescence microscopy. Fluorescence microscope was used to image MCF-7 cells marked with Celltracker Orange and Hoechst for staining the cytoplasm and nucleus, respectively. A single element 375MHz center frequency transducer (SASAM) was used to generate acoustic impedance maps of inverted MCF-7 cells on a plastic substrate. The acoustic impedance of 20 single-live, 10 clustered-live and 7 clustered-fixed MCF7 cells were measured and compared. Fluorescent images and acoustic impedance maps suggest that there is an acoustic impedance mismatch between the nucleus and the cytoplasm. The average acoustic impedance values for single-live, clustered-live and clustered-fixed cancer cells were measured to be 1.600±0.006 MRayl, 1.609±0.009 MRayl and 1.572±0.011 MRayl.**

Keywords: Acoustic impedance maps; Acoustic microscopy; cancer cells.

I. Introduction

Acoustic impedance maps can be used to detect anatomical and physiological changes of cells through identifying changes in their mechanical properties [1-3]. These changes have been used to differentiate between normal and cancerous cells [4]. Understanding the mechanical properties of cancer cells has the potential to improve ultrasound diagnostic capability.

Microscale anatomical structures and their modification can be detected using quantitative ultrasound [3, 5, 6]. Quantitative ultrasound is a technique used to estimate the effective scatterer size and the acoustic scatterer concentration using the frequency analysis of the backscattered signals [5, 6]. Lack of knowledge about the ultrasound scattering source reduced the diagnostic power of quantitative ultrasound. Detecting the ultrasound dominant scattering source can improve quantitative ultrasound technique [7]. Fluctuations in the acoustic impedance maps can be used to gain insight about the dominant ultrasound scattering source of cancer cells [5, 6]. Due to morphological differences between cancer and normal cells (such as the enlarged nucleus of cancer cells), it is thought that quantitative ultrasound techniques can improve ultrasound cancer diagnosis.

In addition, acoustic impedance maps can be used to detect physiological changes [1, 8]. Many physiological changes in the cell e.g. cell division, cell motility, cell adhesion and apoptosis are accompanied by changes in the elastic properties of the cells [2, 9-11]. Elastic properties are directly correlated to the cell acoustic impedance. Measuring the average acoustic impedance, from the acoustic impedance maps can be used to detect physiological changes in cells. However, most acoustic impedance methods developed interrogate the cell using ultrasound beams incident from above the cell. Typically the cell surface is not flat with respect to the interrogating ultrasound wavelength, confounding the interpretation of the data.

Measuring acoustic impedance maps can be performed using a method developed by Hozumi et. al. [12]. This method uses a reference material with a known acoustic impedance to calculate the acoustic impedance of the sample, with the ultrasound beam incident from below the cell. A correction is needed to account for the finite angle of the transducer and the shear waves created in the solid layer [13, 14]. The main purpose of the study is to use this method to calculate, for the first time, the acoustic impedance maps of cancer cells. These maps can be used to gain an insight about the mechanical properties of cancer cells.

II. Sample Preperation

MCF-7 cells, derived from an invasive breast duct carcinoma (ATCC, Manassas, VA), were grown in Dulbecco's modified Eagle's medium (DMEM) and 10% fetal bovine serum (FBS) in an incubator (37^{o}C and 5% CO_2). The cells were passed using trypsin dissociation at 80-90% confluence.

24 hours prior to the experiment the cells were transferred into an Opticell (NUNC Opticell, Thermo Fisher Scientific, Waltham, MA) with 10mL media. The Opticell was left in the incubator for the cells to adhere.

Prior to the experiment, the cytoplasm and the nucleus were fluorescently stained, after they were transferred into the Opticell, using Celltracker Orange (Life Technologies,

Carlsbad, CA) and Hoechst 33342 (Life Technologies, Carlsbad, CA) respectively.

III. Experimental Setup

Figure 1 illustrates the experimental setup used to generate fluorescence images and acoustic impedance maps. Distilled water was used as the coupling fluid. Fluorescent images were taken using a monochrome CCD camera (Lumenera, Ottawa, Ontario, Canada). The radiofrequency signals were acquired using an acoustic microscope (SASAM, Kibero GmbH, Saarbrucken, Germany) kept in a climate controlled chamber at 36.0±0.2 ^{o}C. The pulse generated had a 375MHz center frequency, 150MHz bandwidth, and 60^{o} aperture angle. The radiofrequency signals were obtained by scanning the transducer in the x-y plane (Fig. 1) in 1µm steps scanning a rectangular area of width 40µm-100µm depending on the cell size. Acoustic impedance maps were generated from the maximum peak of the radiofrequency signals as described in [12]. A reference with known acoustic impedance was used to calculate the amplitude of the incident signal (A_0):

$$A_0 = A_r \frac{Z_P + Z_r}{Z_P - Z_r} \quad (1)$$

where A_r is the amplitude of the signal reflected at the polystyrene-reference boundary, Z_P is the acoustic impedance of polystyrene (2.46 MRayl) [14] and, Z_r is the acoustic impedance of the reference. The acoustic impedance of the sample (Z_S) was calculated using:

$$Z_S = Z_P \frac{A_0 - A_S}{A_0 + A_S} \quad (2)$$

where A_S is the amplitude of the signal reflected at the polystyrene-sample boundary. Water was used as a reference to measure the acoustic impedance of media and phosphate buffered saline (PBS). Cells were divided into single or clustered, and live or fixed. Single are cells not attached to other cells and clustered are two or more cells attached to each other. Live cells are not-fixed and fixed are cells fixed with 10% formalin. Media was used as a reference to measure the acoustic impedance of 20 single-live MCF-7 cells and 10 clustered-live MCF-7 cells. PBS was used as a reference to measure the acoustic impedance of 7 clustered-fixed MCF-7 cells.

IV. Data Analysis

Data analysis was performed on acoustic impedance maps to acquire the average acoustic impedance values of single-live, clustered-live and clustered-fixed cancer cells. The image analysis processes applied on the acoustic impedance maps are threshold and erosion. Thresholds were applied to eliminate the background. The threshold values were calculated from the first minima of the smoothed histogram of the acoustic impedance maps (0.005 MRayl average filter size). Erosions were applied to reduce the effect of the transducer point spread function on the measured acoustic impedance values. The erosions were performed using a disk shaped matrix with a diameter of size 3µm (approximate lateral resolution of the transducer). The average acoustic impedance value for each acoustic impedance map was calculated from the non-eliminated pixels. The means and standard deviations were calculated for 20 single-live, 10 clustered-live and 7 clustered-fixed cancer cells. To compare the means, multiple comparison tests were performed on the average acoustic impedance values calculated from each acoustic impedance map with α=0.05 using the post hoc test of Tukey-Kramer).

V. Results

A. Acoustic Impedance maps and fluorecence images

Figure 2 illustrates the acoustic impedance maps of three different MCF-7 cells, and fluorescence microscopy images of the same cells stained with CellTracker Orange (red) and Hoechst (blue). On the right are plots of the different parameters measured at the location of the green trace lines. Black, red and blue represent the normalized acoustic impedance, CellTracker Orange stain and Hoechst stain, respectively. The images demonstrate an increase (Fig. 2a) decrease (Fig. 2b) or no effect (Fig. 2c) on the measured acoustic impedance values of the position correlated with the location of the nucleus when compared to the acoustic impedance values correlated to the location within the cytoplasm.

B. Average acoustic impedance value

The calculated acoustic impedance values for water, media and PBS were measured to be 1.517±0.006 MRayl, 1.549±0.006 MRayl and 1.541±0.006 MRayl, respectively. For MCF-7 cells, the mean acoustic impedance values of single-live, clustered-live and clustered-fixed cells were calculated to be 1.600±0.006 MRayl, 1.609±0.009 MRayl and 1.572±0.011 MRayl respectively as shown in Fig. 3. The means of each cell map were compared using multiple comparison test and the results demonstrate a difference between single-live, clustered-live and clustered-fixed cells.

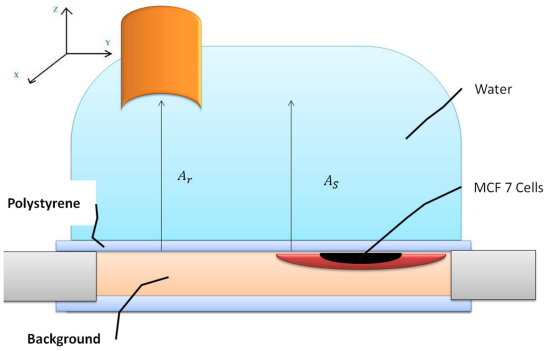

Fig. 1. Schematic setup of the acoustic microscopy.

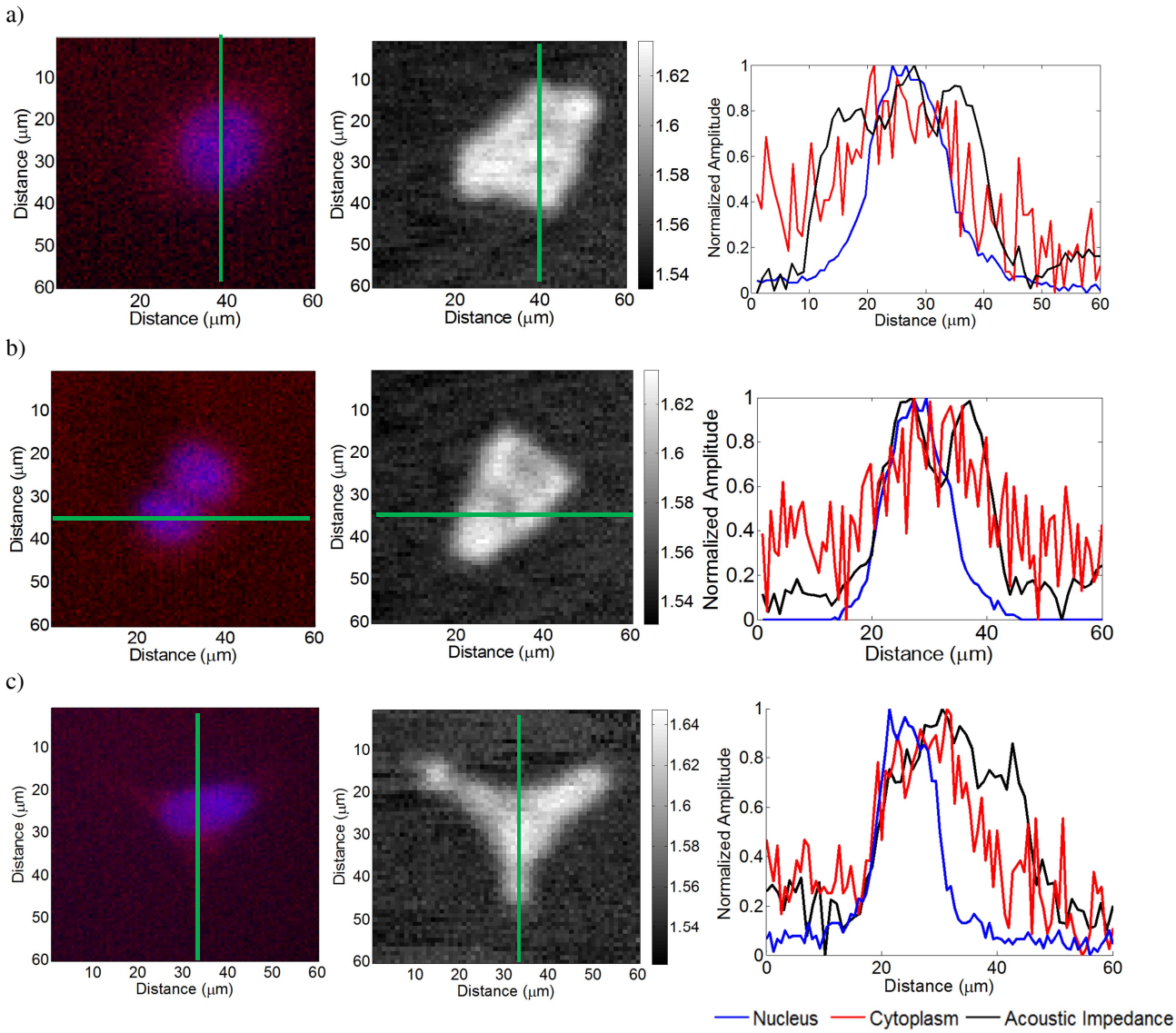

Fig. 2. Comparing acoustic impedance maps with fluorescence images of MCF-7 cells. The left column represents fluorescent images. The middle column represents acoustic impedance maps of the same cells. The right column represent graphs that were acquired at the location denoted with green trace lines of the normalized acoustic impedance (black line), normalized intensity of the Hoechst (blue) and CellTracker Orange stains (red).

VI. Discussion

Using acoustic impedance maps, we were able to identify the nucleus as a fluctuation in the acoustic impedance values when compared to the cytoplasm. The acoustic impedance values increased (Fig. 2a), decreased (Fig. 2b) or did no change (Fig. 2c) at a position correlated to the location of the nucleus when compared to the acoustic impedance values measured in the cytoplasm. These results are likely due to the interference between two waves. The two waves are created from a consecutive acoustic impedance mismatches at a distance shorter than the ultrasound wavelength. The first wave is generated due to the substrate-cytoplasm boundary and the second wave is generated due to the cytoplasm-nucleus boundary. The depth of the nucleus to the substrate will affect the interference of the two waves to create a constructive, destructive, or an interference between these two extremes. This provides insight into ultrasound scattering of biological tissues as the results suggest that the nucleus could be a scattering source due to the detected impedance mismatch between the cytoplasm and nucleus.

To test the accuracy of the method, the acoustic impedance of water was calculated to be 1.517±0.006 MRayl which has a 0.5% error when compared to the known acoustic impedance of water (1.51 MRayl). The average acoustic impedance of single-live cancer cell was calculated to be 1.600±0.006 MRayl, which is higher than 1.56±0.01 MRayl for MCF-7, previously obtained using time-resolved acoustic microscopy [15]. Other investigators, using completely different methods and cell cultures, measured acoustic

impedances of cells to be 1.69 MRayl, 1.74 MRayl and 1.78 MRayl [2, 16, 17].

Comparing the average acoustic impedance of single-live, clustered-live and clustered-fixed cells, using the multiple comparison test, confirms a significant difference between the three means. This confirms that acoustic impedance imaging can be used to detect physiological changes.

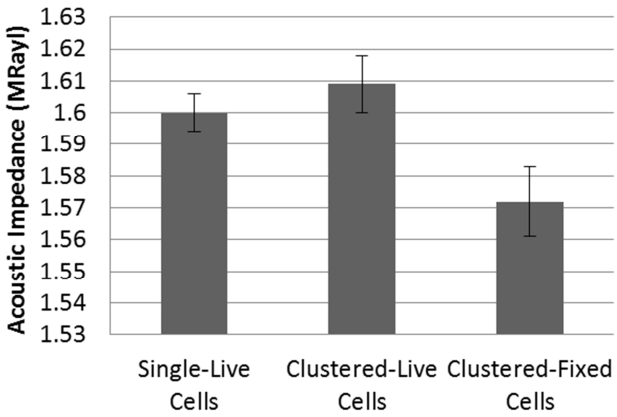

Fig. 3. Results of the mean acoustic impedance values and its standard deviation.

VII. Conclusion

This work presents our measurements of acoustic impedance maps calculated for cancer cells. The acoustic impedance maps were used to detect the nucleus as a fluctuation in the measured acoustic impedance value when compared to the cytoplasm. In addition, the acoustic impedance maps were able to differentiate between single-live, clustered-live and clustered-fixed cells using the calculated average acoustic impedance value.

Acknowledgments

This project was funded by the Natural Sciences and Engineering Research Council of Canada (NSERC) and Terry Fox Foundation. Funding to purchase the equipment was provided by the Canada Foundation for Innovation (CFI).

Reference

[1] S. Suresh, J. Spatz, J. P. Mills, A. Micoulet, M. Dao, C. T. Lim, M. Beil and T. Seufferlein, "Connections between single-cell biomechanics and human disease states: gastrointestinal cancer and malaria," *Acta Biomaterialia,* vol. 1, pp. 15-30, 2005.

[2] E. C. Weiss, P. Anastasiadis, G. Pilarczyk, R. M. Lemor and P. V. Zinin, "Mechanical properties of single cells by high-frequency time-resolved acoustic microscopy," *IEEE Trans. Ultrason. Ferroelectr. Freq. Control,* vol. 54, pp. 2257, 2007.

[3] M. F. Insana, J. G. Wood and T. J. Hall, "Identifying acoustic scattering sources in normal renal parenchyma in vivo by varying arterial and ureteral pressures," *Ultrasound Med. Biol.,* vol. 18, pp. 587, 1992.

[4] M. L. Oelze, J. O'Brien William D., J. P. Blue and J. F. Zachary, "Differentiation and characterization of rat mammary fibroadenomas and 4T1 mouse carcinomas using quantitative ultrasound imaging," *IEEE transactions on medical imaging*, vol. 23, no. 6, pp. 764-771, 2004.

[5] J. Mamou, M. L. Oelze, J. O'Brien William D. and J. F. Zachary, "Identifying ultrasonic scattering sites from three-dimensional impedance maps," *J. Acoust. Soc. Am.,* vol. 117, pp. 413, 2005.

[6] J. Mamou, M. L. Oelze, J. O'Brien William D. and J. F. Zachary, "Extended three-dimensional impedance map methods for identifying ultrasonic scattering sites," *J. Acoust. Soc. Am.,* vol. 123, pp. 1195, 2008.

[7] M. L. Oelze and J. F. Zachary, "Examination of cancer in mouse models using high-frequency quantitative ultrasound," *Ultrasound Med. Biol.,* vol. 32, pp. 1639-1648, 2006.

[8] E. C. Naylor, R. E. B. Watson and M. J. Sherratt, "Molecular aspects of skin ageing," *Maturitas,* vol. 69, pp. 249-256, 2011.

[9] E. Fuchs and K. Weber, "Intermediate Filaments: Structure, Dynamics, Function and Disease," *Annu. Rev. Biochem.,* vol. 63, pp. 345-382, 1994.

[10] G. Bao and S. Suresh, "Cell and molecular mechanics of biological materials," *Nature Materials,* vol. 2, pp. 715-725, 2003.

[11] D. E. Ingber, "Mechanical Signaling and the Cellular Response to Extracellular Matrix in Angiogenesis and Cardiovascular Physiology," *Circulation Research: Journal of the American Heart Association,* vol. 91, pp. 877-887, 2002.

[12] N. Hozumi, A. Kimura, S. Terauchi, M. Nagao, S. Yoshida, K. Kobayashi and Y. Saijo, "Acoustic impedance micro-imaging for biological tissue using a focused acoustic pulse with a frequency range up to 100 MHz," *Ultrasonics Symposium, 2005 IEEE,* vol. 1, pp. 170-173, 2005.

[13] W. G. Mayer, "Energy partition of ultrasonic waves at flat boundaries," *Ultrasonics,* vol. 3, pp. 62-68, 1965.

[14] Hozumi N., Hozumi N., Nakano A., Nakano A., Terauchi S.,Nagao M., Yoshida S., Kobayashi K., Yamamoto S., Saijo Y., "9D-1 precise calibration for biological acoustic impedance microscope," *IEEE Ultrasound Symposium*, pp. 801-804, 2007.

[15] E.M. Strohm, G.J. Czarnota, and M.C. Kolios , “Quantitative measurements of apoptotic cell properties using acoustic microscopy,” *IEEE Trans. Ultrason. Ferroelectr. Freq. Control,* vol. 57, no. 10, pp. 2293-2304, 2010.

[16] T. Kundu, J. Bereiter-Hahn and K. Hillmann, "Measuring elastic properties of cells by evaluation of scanning acoustic microscopy V(Z) values using simplex algorithm," *Biophys. J.,* vol. 59, pp. 1194-1207, 1991.

[17] T. Kundu, J. Bereiter-Hahn and I. Karl, "Cell property determination from the acoustic microscope generated voltage versus frequency curves," *Biophys. J.,* vol. 78, pp. 2270-2279, 2000.